Theoretical Investigations of Intramolecular Energy Transfer Rates and Pathways for Vinyl Bromide on an ab Initio Potential-Energy Surface

Asif Rahaman and Lionel M. Raff*

Department of Chemistry, Oklahoma State University, Stillwater, Oklahoma 74078

Received: May 4, 2000; In Final Form: July 5, 2000

The dynamics of intramolecular energy transfer in vinyl bromide have been investigated using projection methods and results obtained from classical trajectories computed on a global potential-energy surface (PES1) that has been fitted to a large database of energies obtained from ab initio electronic structure calculations at the MP4 level of theory with extended basis sets and experimental thermochemical data. Similar calculations on two additional potential surfaces derived from PES1 are also reported. The intramolecular energy transfer dynamics obtained on these surfaces are compared with one another and with previously reported results using an empirical hybrid-type surface (EPS) fitted to thermochemical, structural, kinetic, and spectroscopic data and the results of a limited number of electronic structure calculations for the transition states. The temporal variation of the average vibrational mode energies are computed from the projected mode kinetic energy profiles using the equipartition theorem. Total energy decay rates and the pathways of energy flow for initial 3.0 eV excitation of each of the 12 vibrational modes in the equilibrium configuration have been determined. The results show that the total relaxation rate for each mode can be characterized with fair accuracy by a first-order rate law. The minimum decay rate among the 12 modes is found to be significantly larger than the decomposition rate for vinyl bromide at an internal energy of 6.44 eV. Such an inequality is a necessary condition to satisfy the basic assumption of statistical theories. However, it is also found that energy transfer is not globally rapid. Some modes are essentially inactive for over one picosecond. Consequently, it is possible that statistical theory will not adequately describe the decomposition processes occurring upon excitation of vinyl bromide. Both the computed energy-transfer pathways and the total mode relaxation rate coefficients are found to be very sensitive to small variations in the surface curvatures near equilibrium and along the reaction coordinates. It is concluded that IVR rates for systems as complex as vinyl bromide computed using trajectory methods and ab initio potentials based on extensive electronic structure calculations will probably yield results with the correct order of magnitude but with errors that can be as large as a factor of 3. The sensitivity of the results to the fine details of surface curvature suggests that if total mode relaxation rates can be accurately measured, they will provide a very demanding test of potential-surface accuracy.

I. Introduction

The study of intramolecular vibrational relaxation (IVR) has a long history spanning approximately three decades. Interest in IVR stems from the close relationship between global IVR rates and the validity of various statistical theories of reaction rates. The fundamental assumption of such theories is that the molecular internal energy is totally randomized on a time scale that is short relative to the reaction rate. Consequently, we are directly concerned with the rate and pathways whereby energy moves from one internal mode to another. In particular, we are interested in the conditions under which global energy randomization can be attained within the time permitted by the rate of the reaction being investigated. In addition, numerous theoretical studies have shown that IVR rates are critically dependent upon the magnitude of the intermode coupling terms in the potential-energy surface and upon the presence of resonance interactions between the internal modes. Therefore, if such mode-to-mode IVR rates can be accurately measured, they will provide sensitive benchmarks against which the accuracy of proposed potential-energy surfaces can be tested.

The calculation of IVR rates is not altogether straightforward. In complex molecules, good internal constants of the motion usually cannot be found. This means that the internal modes are coupled. Under such conditions, it is not clear how to define the energy contained within a particular mode. Such an ambiguity creates obvious problems when attempting to assess IVR rates and pathways. In response, investiagators have developed several theoretical methods that permit useful information to be obtained. Some of these methods employ time-dependent quantum mechanics; others make use of quasiclassical trajectory techniques and some use statistical theories of various types. Regardless of the computational procedure, all methods have as their first prerequisite the development of an accurate potential-energy surface for the system whose IVR rates and pathways are to be studied. In the following discussion, we provide a brief review of these methods, the type of information obtained from their use and some the approximations that have been made to render the problem tractable. As with any such review, no attempt is made to be all-inclusive. Many important contributions will be omitted by space limitations. We intend for this review to do no more than provide a proper context in which to present the results of the present investigation.

One of the first studies of IVR rates was reported by McDonald and Marcus[1]. These investigators used classical methods to compute IVR rates in CD_3Cl and CD_3H. Four different empirical potentials were employed in the study, which

* To whom correspondence should be addressed. Fax: (405) 744−6007

10.1021/jp001696l CCC: $20.00
Published on Web 10/27/2000

indicated that IVR was both global and rapid with complete randomization in less than five picoseconds. A year later, Carter and Brumer[2] used classical trajectory methods to examine IVR rates in vibrationally and rotationally excited planar OCS. An empirical potential-energy surface was developed for this study using methods suggested by Sorbie and Murrell.[3] In this formulation, 16 surface parameters were fitted to the force field obtained by Foord et al.[4] and to experimental binding energies and frequencies for CO, CS and SO. The results showed an exponential divergence of the trajectories and broadened power spectra indicative of classical chaos.

In 1978, Nagy and Hase[5] reported a classical trajectory study of CH overtone decay in benzene using an empirical potential-energy surface with anomalously large force constants for the CCH in-plane wagging mode. The results showed very little decay of the CH overtone states. Three years later, Stannard and Gelbart[6] used quantum mechanical methods to examine IVR for this same system. The Hamiltonian included a zero-order quadratic expression for the modes with empirical coupling terms that did not include any couplings to the ring modes that might have exhibited Fermi resonance with the CH overtone vibrations. Their results were qualitatively in accord with those obtained by Nagy and Hase[5] in that no decay of the initially prepared overtone states of CH was observed.

After the above investigations, Sibert, Reinhardt, and Hynes[7] reported time-dependent quantum calculations of the IVR of CH and CD overtones in benzene and perdeuterobenzene. The potential-energy surface used in their study was a harmonic force field suggested by Pulay et al.[8] In this force field, the mode couplings are represented by quadratic terms. These couplings include interactions between the CH and CD stretches and the ring modes. The stretching modes are simple Morse oscillators with small quadratic cross terms between the various stretching modes. The C−C bonds in the ring are assumed to be rigid, and the effects of rotational motion are ignored. The results of the calculations led to the prediction of broad, unresolved line shapes for C_6H_6 that are consistent with experimental observations. The computed line widths are about 20% to 30% below the measured values. The authors attribute this to rotational broadening that is not considered in the theory. The energy flow from CH or CD overtones to the ring modes was found to be primarily due to the presence of Fermi resonance couplings. Relaxation times were found to vary from 0.062 to 0.160 ps for the $\nu = 5$ to the $\nu = 9$ overtone states. The same authors[9] have also reported the results of classical trajectory calculations for these systems using the same potential-energy surface.[8] Very good agreement between the classical and the time-dependent quantum relaxation rates was obtained. In most cases, the computed relaxation rates were within 20% of one another. This study was of central importance in establishing the capability of classical mechanics to describe IVR.

Once it was understood that classical trajectory studies of IVR dynamics could be expected to yield results in good accord with more exact quantum calculations, numerous such investigations were reported. Uzer, Hynes, and Reinhardt[10,11] used trajectory methods to study the overtone-induced dissociation and IVR in H_2O_2 and HO_2D on a potential surface that incorporated Morse oscillators for the OH, OD, and OO stretches with parameters obtained from a Birge−Spooner analysis of the OH overtone spectrum. The bends were modeled as quadratic terms where the parameters were chosen to fit the measured frequencies. Empirical switching functions were used to incorporate the stretch−bend couplings. These studies indicated that energy randomization is not complete on the time scale of the dissociation reactions.

Bintz, Thompson, and Brady[12] used classical methods to analyze the influence of "bath" modes on IVR rates from a local mode in benzene restricted to remain planar. The potential surface was purely empirical. By varying the potential parameters, it was demonstrated that IVR rates are highly influenced by the extent of the coupling produced by the anharmonicity. Guan and Thompson[13] reported similar calculations on the relaxation of excited normal modes of benzene. Overtones of the C−C stretch, the C−C−H bend, and the C−C−C bend were studied using the semiempirical potential developed by Pulay et al.[8] Only planar motion of benzene was permitted in the computations. Sumpter and Thompson[14] studied the onset of classical chaotic motion in HC_3, HNNH, HCCH, and H_2O_2 using empirical potential surfaces in which Morse potentials represent the stretching potential and simple quadratic functions model the bending potentials. Torsional potentials were incorporated with a truncated Fourier cosine series. It was found that the presence of bending modes lowered the energy at which chaotic motion is observed and increased the IVR rates. Sumpter and Thompson[15] also reported a study of the IVR rate from CH stretching overtones in dimethylnitramine. The major relaxation pathway was found to involve energy transfer from the C−H stretch to the H−C−H bend in the same methyl group followed by excitation of the N-0 stretch and the C−H stretch on the other methyl group.

When the system under investigation contains only a few atoms or when more complex systems are restricted so that their motion is confined to a reduced dimensional framework, it is possible to effectively study IVR and the onset of classical chaotic motion using surfaces of section. Davis and Gray[16] have reported such studies of IVR in HeI_2 whose motion is restricted to a T-shaped geometry containing only two degrees of freedom. Morse potentials are used for I_2 and between He and the I_2 center of mass. Davis[17] has also reported extensive studies using these methods with a model Hamiltonian. The principle result is that even when the system is in an energy regime that is classical chaotic, the quantum local-mode transition does not change significantly so that quantum mechanics is essentially regular. Along these same lines, Kellerman and Chen[18] and Kellerman[19] have investigated IVR in highly excited acetylene using an approximate Hamiltonian containing a zeroth-order part that is diagonal in the normal-mode quantum numbers along with a coupling term consisting of a sum of resonance coupling terms expressed in terms of normal-mode raising and lowering operators. The initial state is prepared with the internal energy residing in the C−H stretching mode. The intramolecular coupling permits the energy to flow into the remaining modes. However, the presence of two near constants of the motion act as bottlenecks to restrict the energy flow and prevent rapid and complete energy randomization. In support, McCoy and Sibert[20] have conducted a perturbation calculation that indicates that approximate constants of the motion exist in C_2H_2.

A particularly useful method for following the evolution of IVR called local frequency analysis has been developed by Martens, Davis, and Ezra,[21] by McDonald and Marcus[1] and by Marcus, Hase, and Swamy.[22] In this method, fast Fourier transforms are performed over short sequential segments of a long trajectory. These transforms provide the temporal variations of the power spectrum bands which can then be directly related to the instantaneous energy transfer rates. Martens et al.[21] have applied the method to the analysis of IVR in a planar model of OCS.

The problem of describing the instantaneous energy present in a given mode has been eliminated by the use of a projection method developed by Raff.[23] In this method, the temporal variations of a diagonal kinetic energy matrix are obtained using trajectory calculations and projection methods. The energy transfer rates and pathways can then be evaluated from the envelop functions of these diagonal elements. This method is described in more detail in Section III of this paper.

The qualitative appearance of the power spectrum has frequently been utilized to monitor the onset of classical chaos and to draw qualitative conclusions concerning the IVR rates. In general, it is observed that as the internal excitation energy and IVR increase, the power spectrum band associated with a given mode frequency broadens and then splits into an ensemble of bands. Agrawal et al.[24] have recently demonstrated that this splitting is a general phenomena that arises because of the continuous frequency modulation produced by intramolecular energy transfer. The splitting effect has, therefore, been called the Continuous Frequency Modulation (CFM) effect. In addition to identifying the cause of the power spectrum splitting, the analysis also shows how quantitatively accurate IVR rates can be extracted from the power spectrum line splittings.

The preceding brief review shows that we currently understand a great deal about the qualitative nature of IVR and have several methods available for studying the dynamics of the process. However, most investigations reported to date have been conducted using purely empirical or semiempirical potential-energy surfaces. In a few cases, hybrid potential surfaces have been developed by combining some quantum electronic structure calculations around the stationary points on the surface with experimental data related to structure, bond energetics, and measured vibrational frequencies. There are no reported investigations of IVR rates and pathways for a complex system containing several possible unimolecular reaction channels that have been carried out using an accurate ab initio potential-energy surface that addresses the energies, curvatures and intramode couplings at most of the important configuration points on the potential surface. Because of this lack, there is no quantitative information related to the effects of surface curvature at the stationary points or along the dissociation coordinate on the computed IVR rates and pathways when the potential-energy surface is a good representation of the experimental surface. The present study reports such an investigation for vinyl bromide. IVR rates for overtone excitation of each of the vinyl bromide normal modes are reported, and the energy transfer pathways for initial excitation of one of the C−H stretching modes are determined using projection methods.[23] The next section reviews previous studies of the vinyl bromide system.

II. Previous Studies of IVR Rates and Pathways in Vinyl Bromide.

The dynamics of intramolecular energy transfer in vinyl bromide have previously been investigated by Pan and Raff[25] using projection methods[23] and results obtained from classical trajectories on a global potential-energy hypersurface. The potential surface was fitted to thermochemical, structural, kinetic, and spectroscopic data and the result of electronic structure calculations for the transition states. Consequently, the potential is a hybrid in that part of the fitting is to empirical data, whereas another part is adjusted to the results of ab initio electronic structure calculations carried out at the MP4 level of theory at stationary points on the surface. In the following discussion, this surface is termed the EPS surface. Total energy decay rates and the pathways of energy flow for initial 3.0 eV excitation of each of the 12 vibrational modes in vinyl bromide were reported.

The results of this study[25] indicated that the total relaxation rate for each mode could be characterized with fair accuracy by a first-order rate law. Least-squares fitting of such a rate law to the computed data gave a minimum decay rate among the 12 modes 3.1 times larger than the total decomposition rate for vinyl bromide at an internal energy of 6.44 eV. Thus, the basic inequality that is a necessary condition for statistical theories of unimolecular reactions to hold was found to be satisfied. However, it was also found that energy transfer on the EPS surface was not globally rapid. Some modes remained inactive for over a picosecond, which significantly exceeds the mean time for unimolecular reaction. Under such conditions, statistical theories may not adequately describe the decomposition processes occurring upon excitation of vinyl bromide.

Pan and Raff[26] also used CFM line splittings[24] to determine energy transfer rate coefficients for the local C−Br and C═C vibrational modes in vinyl bromide and the C−H stretching mode in doubly deuterium-substituted vinyl bromide. In both cases, the EPS potential surface was employed in the calculations. The C−Br and C═C total relaxation rate coefficients computed from the CFM line splittings were found to agree with the corresponding results obtained by projection methods within the combined error limits of the two methods. The C−H relaxation rate coefficients for D_2C═CHBr, *cis*-DHC═CDBr and *trans*-DHC═CDBr are factors of 2.2 to 7.1 smaller than the C−H relaxation rates for vinyl bromide. This difference is expected because the substitution of deuterium for hydrogen removes the near resonance between the three C−H stretching modes in vinyl bromide and thereby significantly reduces the IVR rates.

The fact that the potential surface employed in each of the above investigations is a hybrid that combines semiempirical data and the results of ab initio electronic structure calculations raises questions about the accuracy of the results. There is no doubt that IVR is not globally rapid relative to the unimolecular decomposition rate on the EPS surface. Consequently, we would not expect statistical theories to hold for unimolecular decomposition processes on this surface. This has been found to be the case.[27,28] However, there is little reason to believe that the intermode coupling on the EPS surface accurately reflects that present for the experimental potential surface. The ab initio calculations addressed only the transition-state regions of the potential surface. No calculations related to the effects of coordinate couplings upon the potential were performed. The experimental database to which the potential was fitted included only thermochemical, structural, kinetic, and spectroscopic data, which are only marginally dependent upon intermode coupling. Therefore, the question of IVR rates in vinyl bromide remains open as does the question of how accurately hybrid and empirical surfaces can be expected to describe intramolecular energy transfer rates and pathways. This latter question has significance beyond the vinyl bromide system because most theoretical calculations of IVR rates have been executed using such empirical, semiempirical, or hybrid surfaces[1−22,25,26].

Rahaman and Raff[29] have recently reported the development of an ab initio, global potential-energy hypersurface for vinyl bromide. The fully relaxed MP4 energies with all single, double, and triple excitations included were determined at 299 different nuclear conformations using a 6-31G(d,p) basis set for carbon and the hydrogen atoms and Huzinaga's[30] (4333/433/4) basis set augmented with split outer s and p orbitals to yield (43321/

4321/4) and a polarization f orbital with an exponent of 0.5 for the bromine atom. These calculations focused upon the determination of the dependence of the potential upon the stretching coordinates for the bonded atoms, the C−C−H and C−C−Br bending coordinates, and the dihedral angles. Extensive calculations were also carried out to determine the couplings between these coordinates. The total ab initio database to which the global function is fitted was obtained by combining the results of the above calculations with previously reported studies[31−34] of the vinylidene-acetylene system and ab initio computations of the saddle-point geometries and energies for the various decomposition channels.[28] This provides a database of about 400 points to which analytic functions can be fitted to produce an ab initio potential for vinyl bromide. We have labeled this potential PES1. It is fully described in ref 29.

The accurate investigation the dependence of IVR rates and pathways upon potential-surface curvatures is difficult when the potential-surface is a highly coupled representation of the true experimental surface for a system as complex as vinyl bromide. We cannot simply change one or more of the surface parameters that have been fitted to the ab initio database via nonlinear least-squares procedures and then repeat the calculations of IVR rates and pathways to determine the changes produced. Such a procedure will tell us what variations in the IVR rates and pathways are introduced, but it will be impossible to assign those variations to any one particular topographical feature of the potential because a change in one or more of the potential parameters will produce numerous variations in the topology of the surface due to the highly coupled nature of the potential. To unequivocally assign a computed variation in the IVR rate or energy transfer pathway to a given change a particular topographical feature of the potential surface that feature must be the only difference between the two potentials used in the calculations. Consequently, if such a determination is to be made, it requires the development of a series of potential surfaces in which given topographical features are varied one at a time in a known manner. The development of such a sequence of surfaces is a laborious procedure requiring repeated iteration and careful monitoring of the total surface topology. Even when this is done, the extent to which a single feature of a surface can be altered without producing other simultaneous topographical variations is limited.

Rahaman and Raff[29] have reported the development of two potentials surfaces, PES2 and PES3, that are derivative surfaces of the ab initio PES1 surface. PES2 is obtained by iterative adjustment of the equilibrium curvature parameters so as to force better agreement between the vinyl bromide fundamental frequencies predicted by the surface and those obtained from IR and Raman measurements. At the same time, other surface parameters are varied so as to maintain the remaining important topographical features of the potential as constant as possible. Once completed, the parameter values for PES2 are varied iteratively to arbitrarily decrease the curvatures along the three-center HBr and H_2 elimination reaction coordinates, whereas at the same time maintaining other features of the potential unchanged. The resulting potential is labeled PES3. The parameters values and other features of each of these surfaces are fully described in Reference 29. By comparing computed IVR rates and pathways on PES2 and PES3 with those obtained using PES1, we may quantitatively evaluate the importance of equilibrium and reaction coordinate curvatures upon the energy transfer and reaction dynamics. A further comparison between IVR dynamics on these surfaces with those obtained using the EPS surface provides quantitative information related to the reliability of computations carried out on such hybrid potential-energy surfaces.

A detailed investigation of the vinyl bromide decomposition dynamics on PES1, PES2, PES3, and EPS surfaces has been reported by Rahaman and Raff.[29] These investigations included computation of the total decomposition rate coefficients and product branching ratios as a function of excitation energy, the vibration-energy distribution of HBr molecules formed via three-center HBr elimination reactions at 6.44 eV excitation energy and the detailed mechanisms for three-center HBr and H_2 elimination reactions. Comparison of the results obtained on the four potential surfaces among themselves and with the available experimental data led the Authors to conclude that while useful information related to polyatomic reaction dynamics can be obtained by employing empirical surfaces, it is necessary to exercise great care when proceeding in this fashion. It is possible that the results may not even be qualitatively correct. It was also concluded that small variations in the potential surface curvatures at equilibrium and along the reaction coordinates do not exert major influence upon the reaction dynamics.

In this paper, we report the results of theoretical studies of the intramolecular energy transfer rates among the 12 vibrational modes of vinyl bromide for initial 3.0 eV excitation of each of the modes. Calculations are performed on PES1, PES2, and PES3. The results so obtained are compared among themselves and with previously reported IVR rates using the EPS potential surface.[25,26] In Section III, we provide a brief review of the projection method and the associated numerical procedures for the investigation of intramolecular energy transfer. The results of the calculations are given in Section IV. Section V summarizes the important conclusions and results.

III. Projection Method and Numerical Procedures

Projection Method. The projection method[23] is based on the calculation of the temporal variation of a diagonal kinetic energy matrix. The energy transfer rates and pathways are extracted from the envelope functions of this temporal variation. Because the potential energy is not involved in the analysis, all problems associated with potential coupling between the vibrational modes are eliminated. The basis of the method is reviewed below.

Let $\boldsymbol{L_i}$ ($\boldsymbol{i} = 1,2,3,...,3N$) represent a set of normalized ($3N \times 1$) transformation vectors that project the normal mode vibrations, $\boldsymbol{Q_i}$ ($1 \le i \le 3N - 6$), the center-of-mass translations, $\boldsymbol{Q_i}$ ($3N - 5 \le i \le 3N - 3$), and the rotations about the molecular center-of-mass, $\boldsymbol{Q_i}$ ($3N - 2 = i = 3N$) onto the Cartesian displacements, q_j ($j = 1,2,3,...,3N$). At time t, the instantaneous Cartesian velocities may, therefore, be written as linear combinations of the elements of $\boldsymbol{Q_i}$

$$\dot{q}_i(t) = \sum_{j=1}^{3N} \dot{Q}_j(t) L_{ij} \text{ for } i = 1,2,3,...,3N \qquad (1)$$

Equation 1 may be written in matrix form as

$$\dot{\boldsymbol{q}}(t) = \boldsymbol{L}\dot{\boldsymbol{Q}}(t) \qquad (2)$$

where $\boldsymbol{L}$ is a ($3N \times 3N$) square matrix whose columns are the normalized projection vectors, $\boldsymbol{L_i}$. $\dot{\boldsymbol{q}}(t)$ is a ($3N \times 1$) column vector whose elements are the Cartesian velocities, and $\dot{Q}(t)$ is a ($3N \times 1$) column vector whose elements are the normal mode, center-of-mass, and rotation velocities. The normal mode

velocities are, therefore, given by

$$\dot{\boldsymbol{Q}}(t) = \boldsymbol{L}^{-1}\boldsymbol{q}(t) \tag{3}$$

The kinetic energy T at time t is

$$T(t) = 0.5\sum_{i=1}^{3N} m_i q_i^{\,2}(t) \tag{4}$$

Substitution of eq 1 yields

$$T(t) = 0.5\sum_{i=1}^{3N} m_i \sum_{j=1}^{3N}\sum_{k=1}^{3N} \dot{Q}_j(t)\dot{Q}_k(t)L_{ij}L_{ik} = 0.5\sum_{i=1}^{3N} mi \sum_{j=1}^{3N} \dot{Q}_j^{\,2}(t)L_{ij}^{\,2} \tag{5}$$

because the kinetic energy is diagonal when expressed in terms of the normal mode velocities. Consequently, the kinetic energy may be written as

$$T(t) = \sum_{j=1}^{3N} a_j \dot{Q}_j^{\,2}(t) \tag{6}$$

provided the mode constant a_j is defined to be

$$a_j = 0.5\sum_{i=1}^{3N} m_i L_{ij}^{\,2} \tag{7}$$

Equation 6 shows that the total molecular kinetic energy is the uncoupled sum of the individual mode kinetic energies, $T_i(t)$, where

$$T_i(t) = a_i \dot{Q}_i^{\,2}(t) \tag{8}$$

The total energy associated with a given mode alternates between potential and kinetic energy with a frequency characteristic of the mode fundamental. If there is no energy flow to or from the mode, the envelope of these oscillations will have a zero slope. A rapid energy transfer, however, will produce a large slope to the envelope function. Thus, the energy flow through the molecule may be determined directly from the temporal variations of the envelopes of the mode kinetic energies.

Because the average kinetic energy is one-half of the total energy, we may compute an approximate average total energy associated with a given mode i from

$$< E_i(t) > = 2(\Delta t)^{-1}\int_{t_0}^{t_0+\Delta t} T_i(t)\mathrm{d}t = 2(\Delta t)^{-1}\int_{t_0}^{t_0+\Delta t} a_i \dot{Q}_i^{\,2}(t)\mathrm{d}t \tag{9}$$

where t is a time in the interval $t_0 \le t \le t_0+\Delta t$. The time interval Δt is chosen to average out most of the fluctuations in $T_i(t)$ due to beats and the interconversion of potential and kinetic energies within the same mode.

If the initial excitation energy is inserted into mode i, the temporal variation of $<E_i(t)>$ is directly related to the rate of energy flow out of this mode. In this and previous studies,[25,26] we have assumed that this energy flow can be adequately described by a first-order rate law. Although this assumption is not rigorously correct, it will be seen that it is sufficiently accurate to permit us to determine in a semiquantitative fashion the nature of IVR in vinyl bromide. Under these conditions, the total intramolecular energy transfer rate coefficient k_i can be deduced by fitting the equation

$$<E_i(t)> = E_i(0)\exp[-k_i t] + (1 - \exp[-\alpha_i t])\ <E_i(\infty)> \tag{10}$$

to the data obtained from eq 9. In eq 10, k_i, α_i and $<E_i(8)>$ are parameters representing the total relaxation rate coefficient of mode i, an average total rate coefficient for energy transfer into mode i and the statistical equilibrium value of $<E_i(t)>$ at infinite time, respectively.

Numerical Procedures. Initially, vinyl bromide is placed in the equilibrium conformation predicted by the global surface.[29] Zero-point vibrational energy is inserted into each of the vinyl bromide normal modes using eq 1 with the $\dot{Q}_i(t)$ for rotations and translations set to zero. Hamilton's equations of motion are then integrated for a randomly chosen period t_p given by

$$t_p = \xi\tau \tag{11}$$

where ξ is a random number selected from a distribution that is uniform on the interval [0,1], and τ is the characteristic period of the lowest frequency vibrational mode in vinyl bromide. The numerical integrations are effected using a fourth-order Runge−Kutta procedure with a fixed step size of 0.01 t.u. (0.000 101 9 ps). Equation 11 effectively averages over the vibrational phases of the lattice. After the above integration, the desired excitation energy, E_{ex}, is inserted into the selected mode k. This is accomplished by first using eq 3 to project out the instantaneous normal mode velocities, $\dot{\boldsymbol{Q}}_i(t_p)$. The velocity $\dot{\boldsymbol{Q}}_k(t_p)$ is then altered to $\dot{Q}'_k\ (t_p)$ to reflect the insertion of the excitation energy E_{ex}. The required velocity is given by

$$\dot{Q}'_k(t_p) = \pm\ \{(a_k)^{-1}[a_k\ \dot{Q}_k^2(t_p) + E_{ex}]\ \}^{1/2} \tag{12}$$

where the sign is chosen randomly. The new Cartesian velocities are computed using eq 1. In the present investigation, E_{ex} has been taken to be 3.0 eV.

The subsequent dynamical behavior of the system is followed for a period of 450 t.u. (4.586 ps) to determine the nature of the energy transfer. After every tenth integration step, eq 3 is used to compute the instantaneous values of the $\dot{Q}_i(t)$ (i = 1,2,3,...,3N). The mode kinetic energies are calculated using eq 8. Approximate average mode energies at time t^* are obtained from eq 9 using Δt = 25 t.u. (0.255 ps) and $t^* = t_o + \Delta t/2$. Four significant digits of energy conservation is generally achieved.

IV. Results and Discussion

Table 1 gives a qualitative description of each of the vibrational modes of vinyl bromide. It also lists the computed normal-mode frequencies of these modes on each potential surface along with the experimentally measured values.

To provide direct comparisons with the energy transfer dynamics obtained using the hybrid empirical EPS surface, we have executed calculations on PES1, PES2, and PES3 equivalent to those reported in ref 25. After preparation of the initial vinyl bromide state using the methods described in the previous section, 3.00 eV of excitation energy is partitioned into the C−H stretching mode ν_{10} using eqs 1 and 12. The intramolecular energy flow in vinyl bromide is then determined using projection techniques.

Figure 1A−1D show the temporal variations of the kinetic energies in each of the vinyl bromide vibrational modes after the 3.0 eV excitation of ν_{10} when the potential-energy surface

TABLE 1: Descriptions of the Vinyl Bromide Vibrational Modes, Their Computed Fundamental Vibrational Frequencies Expressed in Wave Numbers on the Four Potential-Energy Surfaces, and the Measured Values of These Frequencies

		fundamental vibrational wave numbers (cm^{-1})				
mode	description	PES1[a]	PES2[a]	PES3[a]	EPS[b]	expt
ν_1	C−C−Br bend	335	340	340	345	344
ν_2	CHBr wag	581	570	571	576	583
ν_3	C−Br stretch	593	603	603	623	613
ν_4	CH_2 wag	986	902	902	889	902
ν_5	CH_2−CHBr torsion	1053	953	953	963	942
ν_6	C−C−H^5 bend[c]	1130	1022	1022	1004	1006
ν_7	C−C−H^3 bend[c]	1142	1231	1231	1214	1256
ν_8	H−C−H bend	1375	1396	1396	1377	1373
ν_9	C═C stretch	1765	1603	1603	1606	1604
ν_{10}	C−H stretch	3386	3015	3008	3004	3027
ν_{11}	C−H stretch	3478	3087	3085	3086	3086
ν_{12}	C−H stretch	3520	3135	3136	3121	3113

[a] ref 29. [b] ref 28. [c] The superscripts identify the hydrogen atom in vinyl bromide according to the notation used in Reference 28. H^5 is the $-CH_2$ hydrogen cis to the −CHBr hydrogen atom that is denoted by H^3.

is PES1. Inspection of the kinetic energy in mode 10 reveals that the envelope function decreases rapidly to near equilibrium levels in about 30 t.u. (0.3 ps), indicating a very rapid total energy transfer rate out of this mode. The primary pathways for energy transfer from ν_{10} can be easily determined from the results shown in Figure 1. Examination of the kinetic energy variations for each of the remaining eleven modes shows that only ν_{12} has a kinetic energy amplitude that increases rapidly over the first 4 t.u. (0.041 ps). Therefore, the major energy transfer path is $\nu_{10} \rightarrow \nu_{12}$. Table 1 shows these modes to be in near resonance so the prominence of this transfer pathway is not surprising.

Around 7 t.u. (0.071 ps) into the trajectory, energy begins to flow into the third C−H stretching mode, ν_{11}, and into the H−C−H bending mode, ν_8. The transfer pathways involved in this transfer could be $\nu_{10} \rightarrow \nu_{11}$ and ν_8 or they could be $\nu_{12} \rightarrow \nu_{11}$ and ν_8. It is possible that both pathways are present. The data do not provide a definitive answer to this question.

After energy transfer into modes 8 and 11 around 10 t.u. (0.102 ps), the kinetic energy in mode 6, the C−C−H^5 bend, begins to increase. The C═C stretch (ν_9) and the C−C−H^3 bending mode (ν_7) also gain energy at this time. The failure of these modes to initially gain energy from the C−H stretching modes suggests that the coupling is primarily between ν_8 and ν_{11} rather than with modes 10 or 12. Consequently, these transfers are tertiary pathways in the IVR process.

Around 20 t.u. (0.204 ps), the kinetic energy in the CH_2 wag (ν_4) and the C−Br stretch (ν_3) begins to increase. Therefore, we may identify these excitations as being quaternary pathways in which the primary energy transfer is from modes 6, 7, and 9. Only after 60 t.u. (0.611 ps) have elapsed, do we observe energy being transferred into the C−C−Br bend (ν_1), the CHBr wag (ν_2) and the CH_2−CHBr torsion (ν_5). These delayed transfer processes are probably due to the coupling of these modes with the CH_2 wag and the C−Br stretch.

Qualitative examination of the kinetic energy envelope function for the C−C−Br bend(ν_1) in Figure 1A clearly shows that the overall energy transfer, although fast, is not globally rapid. This mode remains nearly inactive throughout the trajectory. Considering the large frequency difference between this mode and the remaining modes in vinyl bromide, this is not a particularly surprising result.

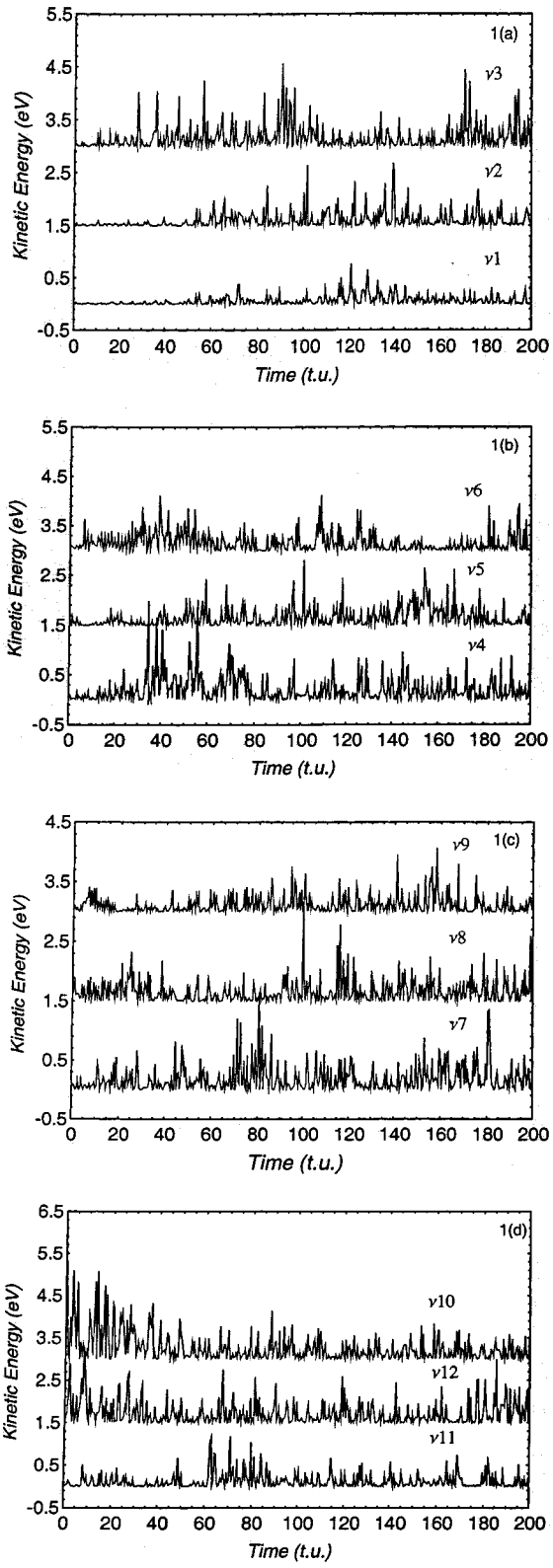

Figure 1. Temporal variations of the mode kinetic energies on PES1 for the 12 vinyl bromide vibrational modes computed using eq 8 for the case in which 3.0 eV of excitation energy in excess of zero-point energy is initially partitioned into the C−H stretching mode ν_{10}. Each successive curve is displaced upward by 1.50 eV to provide visual clarity. The abscissa unit is 1 t.u. = 0.010 19 ps. (A) Modes ν_1, ν_2, and ν_3; (B) Modes ν_4, ν_5, and ν_6; (C) Modes ν_7, ν_8, and ν_9; (D) Modes ν_{10}, ν_{11}, and ν_{12}.

Similar investigations have been conducted on the PES2 and PES3 potentials. Figure 2A−2D show the results on PES2. This surface differs from the ab initio PES1 surface primarily in the

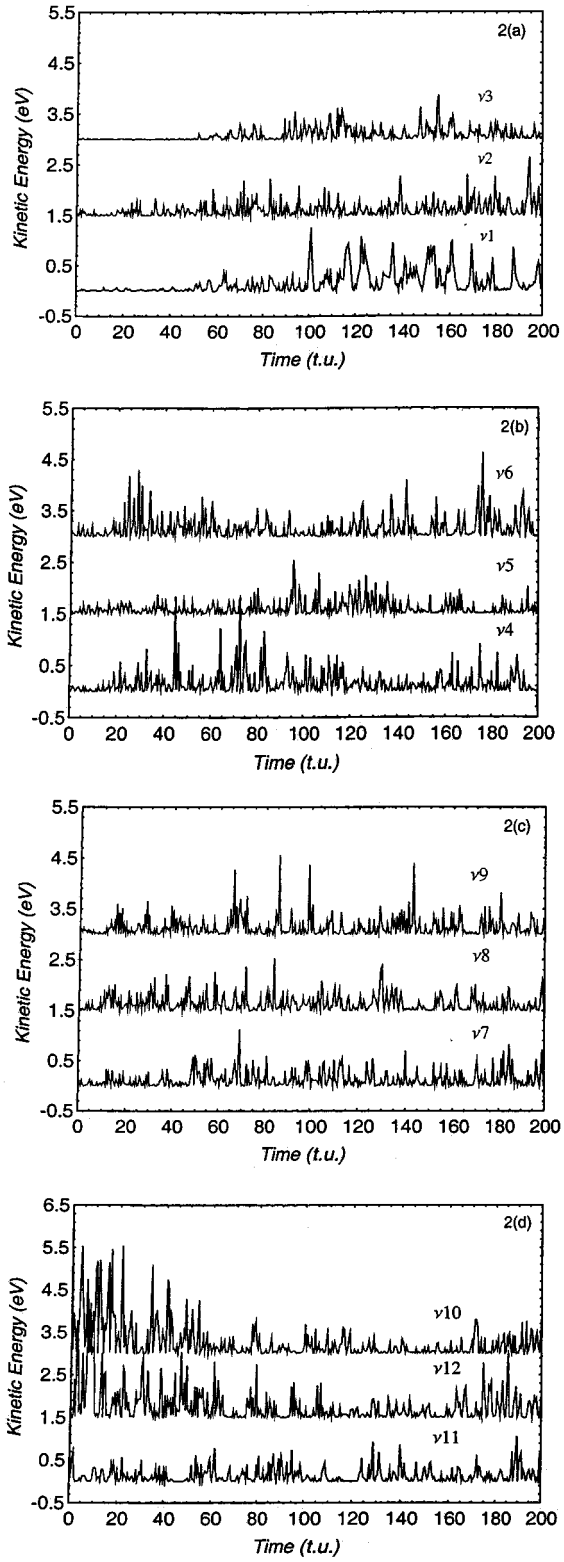

Figure 2. Temporal variations of the mode kinetic energies on PES2 for the 12 vinyl bromide vibrational modes computed using eq 8 for the case in which 3.0 eV of excitation energy in excess of zero-point energy is initially partitioned into the C−H stretching mode ν_{10}. Each successive curve is displaced upward by 1.50 eV to provide visual clarity. The abscissa unit is 1 t.u. = 0.010 19 ps. (A) Modes ν_1, ν_2, and ν_3; (B) Modes ν_4, ν_5, and ν_6; (C) Modes ν_7, ν_8, and ν_9; (D) Modes ν_{10}, ν_{11}, and ν_{12}.

predicted fundamental vibrational frequencies for vinyl bromide. The equilibrium curvature parameters in PES1 were varied so as to obtain better agreement between the predicted frequencies and those obtained in Raman and IR measurements. Some of the switching parameters are also varied to maintain all other topographical features of the PES1 potential as constant as possible. Because the curvature of the potential surface controls, in large measure, the mode-to-mode coupling, we might expect the frequency adjustment to produce significant changes in the magnitude and directions of energy relaxation.

Examination of the kinetic energy envelope functions over the first 10 t.u. (0.102 ps) shows that the primary transfer pathway is from mode 10 to mode 12 as it is for PES1. After 10 t.u., the kinetic energy of the third C−H stretch, mode 11, begins to increase as does that for modes 7, 8 and 9. This is very similar to the results obtained using PES1. However, excitation of the $C-C-H^5$ bending mode (ν_6) is now delayed. On PES2, this mode does not exhibit significant excitation until 20 t.u. (0.204 ps) have passed. The secondary transfer process on this potential appear to be $\nu_{12} \rightarrow \nu_{11,}$ ν_7, ν_8 and ν_9.

At approximately 20 t.u., energy transfer into modes 4 and 6 is observed. The inference is that this excitation energy must have been transferred from modes 7, 8, 9 and 11 because no transfer was observed when only modes 10 and 12 contained the majority of the excitation energy. After 60 t.u. (0.611 ps), we see modes 1, 2, 3, 5, and 7 begin to gain energy. These quaternary transfers presumably involve the CH_2 wag (ν_4) and the $C-C-H^5$ bend (ν_6).

Comparison of the kinetic envelope function for the C−Br stretching mode (ν_3) with those for the remaining modes shows that the overall energy transfer is not globally rapid on PES2. Qualitatively, this is identical to the result for PES1. However, the energy bottleneck on PES2 is primarily the C−Br stretch rather than the C−C−Br bend as is the case for PES1.

Table 2 compares the qualitative energy transfer pathways observed on PES1, PES2, PES3, and the EPS surfaces. Let us first examine the results on the two ab initio surfaces, PES1 and PES2, that differ only in small adjustments of the equilibrium curvatures on PES2 to produce 5 to 10% improvement in the fundamental frequencies. The primary transfer process on both surfaces is $\nu_{10} \rightarrow \nu_{12}$. The secondary processes are also similar. However, the excitation of modes 7 and 9 appears to be secondary on PES2, whereas it is tertiary on PES1. Energy transfer into the $C-C-H^5$ bend (ν_6) is a tertiary process on both PES1 and PES2. However, the CH_2 wag (ν_4) receives energy in a tertiary process on PES2 but in a quaternary pathway on PES1. Beyond this point, the two surfaces show significant differences with the energy transfer to the remaining modes being faster on PES2 than is the case on PES1. These results indicate that very small alterations of the surface curvatures near equilibrium can produce variations in the intramode couplings that alter the qualitative importance of different paths of energy transfer. Because these curvatures are extremely difficult to obtain with an error of less than 5% using ab initio methods, it appears that our presently available computational facilities and methods are insufficient to permit the fine details of IVR to be elucidated with confidence. In contrast, the computed unimolecular dissociation dynamics and mechanisms did not exhibit such pronounced sensitivity.[29]

The results obtained using PES3 underscore the above point. In this surface, the reaction coordinate curvatures are decreased by a small amount to permit the study of the effects of such topographical variations.[29] When such changes are made, the differences between the results and those obtained using PES1 become ever greater. The CH_2 wag (ν_4) is excited in a secondary process on PES3 whereas this excitation occurs much later on PES1 in a quaternary transfer. The CHBr wag (ν_2) and the torsional mode (ν_5) gain energy in a tertiary process on PES3.

TABLE 2: Qualitative Description of Energy Transfer Pathways in Vinyl Bromide Subsequent to Excitation of the C−H Stretching Mode ν_{10} with 3.0 eV of Energy

potential surface	PES1[a]	PES2[a]	PES3[a]	EPS[b]
primary processes	$\nu_{10} \rightarrow \nu_{12}$	$\nu_{10} \rightarrow \nu_{12}$	$\nu_{10} \rightarrow \nu_{12}$ $\nu_{10} \rightarrow \nu_{12}$	$\nu_{10} \rightarrow \nu_{11}$ $\nu_{10} \rightarrow \nu_{11}$
secondary processes	$(\nu_{10}, \nu_{12}) \rightarrow \nu_{11}$ $(\nu_{10}, \nu_{12}) \rightarrow \nu_8$	$(\nu_{10}, \nu_{12}) \rightarrow \nu_{11}$ $\nu_{12} \rightarrow \nu_7, \nu_8, \nu_9$	(ν_{11}, ν_{12}) $\rightarrow \nu_4, \nu_7, \nu_8$	$(\nu_{10}, \nu_{11}, \nu_{12}) \rightarrow \nu_4$
tertiary processes	$(\nu_8, \nu_{11}) \rightarrow \nu_6$ $(\nu_8, \nu_{11}) \rightarrow \nu_7$ $(\nu_8, \nu_{11}) \rightarrow \nu_9$	$(\nu_7, \nu_8, \nu_9, \nu_{11}) \rightarrow \nu_4$ $(\nu_7, \nu_8, \nu_9, \nu_{11}) \rightarrow \nu_6$	$(\nu_4, \nu_7, \nu_8) \rightarrow \nu_2$ $(\nu_4, \nu_7, \nu_8) \rightarrow \nu_5$ $(\nu_4, \nu_7, \nu_8) \rightarrow \nu_6$ $(\nu_4, \nu_7, \nu_8) \rightarrow \nu_9$	$\nu_4 \rightarrow \nu_3$ $\nu_4 \rightarrow \nu_5$
quaternary processes	$(\nu_6, \nu_7, \nu_9) \rightarrow \nu_3$ $(\nu_4, \nu_7, \nu_9) \rightarrow \nu_4$	$(\nu_4, \nu_6) \rightarrow \nu_1$ $(\nu_4, \nu_6) \rightarrow \nu_2$ $(\nu_4, \nu_6) \rightarrow \nu_3$ $(\nu_4, \nu_6) \rightarrow \nu_5$ $(\nu_4, \nu_6) \rightarrow \nu_7$	$(\nu_2, \nu_5, \nu_6, \nu_9) \rightarrow \nu_1$ $(\nu_2, \nu_5, \nu_6, \nu_9) \rightarrow \nu_3$	$(\nu_3, \nu_5) \rightarrow \nu_1$ $(\nu_3, \nu_5) \rightarrow \nu_2$ $(\nu_3, \nu_5) \rightarrow \nu_6$ $(\nu_3, \nu_5) \rightarrow \nu_8$ $(\nu_3, \nu_5) \rightarrow \nu_9$

[a] ref 29. [b] ref 28.

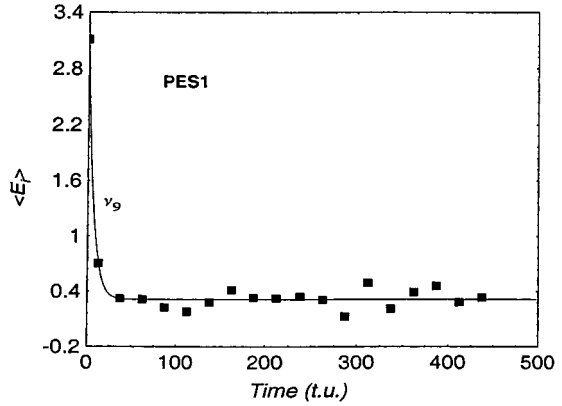

Figure 3. Exponential decay curve for the average mode energy for initial excitation of the C═C stretching mode, ν_9, with 3.0 eV in excess of zero-point energy. The points are computed using eqs 8 and 9. The solid line is the predicted first-order result obtained by least-squares fitting of eq 10 to the points. The abscissa unit is 1 t.u. = 0.010 19 ps.

On PES1, these excitations occur beyond even quaternary processes. Again, the computed unimolecular dissociation dynamics[29] are not found to be extremely sensitive to small variations in the reaction coordinate curvatures.

When the energy transfer pathways on PES1 are compared with those obtained using the empirical EPS surface,[25,28] significant qualitative differences are seen. However, it should be noted that while the more intimate details of intramolecular energy transfer are very sensitive to the fine details of the potential-surface curvatures, the gross behavior of the energy transfer dynamics is not. On all potential surfaces, the primary transfer processes are essentially the same, and in all cases, the total energy transfer rate is found to be fast, but not globally fast relative to the unimolecular dissociation rates of vinyl bromide. Consequently, we expect to see significant deviations from statistical theory on each of the surfaces investigated in these studies.

The total relaxation rate of each of the vinyl bromide vibrational modes with 3.0 eV of excitation energy has been obtained using eqs 8 and 9 to compute approximate mode energies as a function of time and eq 10 to fit the results to a first-order rate law. Typical results are shown in Figure 3 for the C═C stretching mode ν_9 on the PES1 potential surface. It is evident that the major features of the energy transfer are sufficiently well described by the first-order model to make it a useful tool for the presentation of data in succinct form. Qualitatively similar results have been previously reported for the EPS surface.[25]

TABLE 3: Total IVR Rate Coefficients Computed by Least-squares Fitting of eq 10 to the Results Obtained Using eqs 8 and 9 on the PES1 Potential Surface[a]

mode	k_i (ps^{-1})	α_i (ps^{-1})	$\langle E_i(0) \rangle$ (eV)	$\langle E_i(\infty) \rangle$ (eV)
ν_1	8.636	7.949	3.0484	0.2965
ν_2	5.201	6.183	3.0637	0.2907
ν_3	15.996	1.668	3.0644	0.3220
ν_4	20.903	4.612	3.0830	0.3898
ν_5	5.986	6.084	3.0858	0.4236
ν_6	7.556	186.457	3.0889	0.3474
ν_7	17.272	3.729	3.0893	0.3791
ν_8	4.220	1.668	3.980	0.3254
ν_9	15.505	15.898	3.111	0.3135
ν_{10}	7.556	7.458	3.1538	0.3410
ν_{11}	13.739	187.144	3.1559	0.4357
ν_{12}	10.010	9.617	3.1568	0.2842

[a] In each case, 3.0 eV of energy in excess of zero-point energy is initially partitioned into the indicated vibrational mode using the projection method described in the text.

TABLE 4: Comparison of Total IVR Rate Coefficients Computed by Least-squares Fitting of eq 10 to the Results Obtained Using eqs 8 and 9 on the PES1, PES2, PES3, and EPS Potential Surfaces[a]

	k_i (ps^{-1})			
mode	PES1	PES2	PES3	EPS
ν_1	8.636	8.734	9.028	8.7
ν_2	5.201	29.637	18.548	15.9
ν_3	15.996	8.243	8.243	17.0
ν_4	20.903	21.590	48.577	18.6
ν_5	5.986	17.076	19.333	24.5
ν_6	7.556	18.531	25.417	14.2
ν_7	17.272	8.538	12.561	14.2
ν_8	4.220	9.715	4.514	17.8
ν_9	15.505	10.697	18.548	14.2
ν_{10}	7.556	5.496	18.449	13.1
ν_{11}	13.739	4.122	5.201	6.5
ν_{12}	10.010	5.790	19.823	16.5

[a] In each case, 3.0 eV of energy in excess of zero-point energy is initially partitioned into the indicated vibrational mode using the projection method described in the text.

Table 3 summarizes the vibrational relaxation data for each mode on the ab initio PES1 potential. Table 4 compares the total relaxation rate coefficients for each mode on the PES1, PES2, PES3, and EPS surfaces. It is clear that significant quantitative differences exist between the computed total relaxation rate coefficients on the four surfaces. This is true even for PES1, PES2, and PES3, all of which are primarily ab initio surfaces. The only differences are 5 to 10% variations in the equilibrium and reaction coordinate potential curvatures.

These small differences can produce as much as a 350% variation in the total relaxation rate coefficient. This sensitivity and the variation of results shown in Table 4 suggest that the absolute accuracy of IVR rates computed using trajectory methods for systems of this complexity or greater is likely to be less than a factor of 4. It also means that if total mode relaxation rates can be accurately measured, the results will provide a very demanding test of potential-surface accuracy.

When viewed from another perspective, the results shown in Table 4 are encouraging. In most complex systems, total mode relaxation rates cannot be experimentally measured. Even in the most favorable cases, such relaxation rates are obtained with an accuracy that is probably less than a factor of 2 or three. The present results combined with those previously reported[25] show that empirical potential surfaces whose formulation is based upon a limited number of ab initio calculations along with experimentally determined activation energies, product and reactant equilibrium geometries, fundamental frequencies, and heats of reaction are capable of yielding energy transfer rates with errors of a factor of 4 or less. Therefore, the error is approximately the same as that present in the experiments.

V. Summary

The dynamics of intramolecular energy transfer in vinyl bromide have been investigated using projection methods and results obtained from classical trajectories computed on a global potential-energy surface (PES1) that has been fitted to a large database of energies obtained from ab initio electronic structure calculations at the MP4 level of theory with extended basis sets and experimental thermochemical data.[29] Similar calculations on two additional potential surfaces derived from PES1 are also reported. The first of these (PES2) introduces small alterations in the potential-energy curvatures near equilibrium so as to produce 5−10% improvements in the predicted fundamental vibrational frequencies of vinyl bromide. The second surface (PES3) incorporates additional small, arbitrary variations in the reaction coordinate curvatures to permit the effects of this aspect of surface topology to be investigated. The intramolecular energy transfer dynamics obtained on all surfaces are then compared with one another and with previously reported results using an empirical hybrid-type surface (EPS) fitted to thermochemical, structural, kinetic, and spectroscopic data and the results of a limited number of electronic structure calculations for the transition states.[25,28]

The temporal variation of the average vibrational mode energies are computed from the projected mode kinetic energy profiles using the equipartition theorem. Total energy decay rates and the pathways of energy flow for initial 3.0 eV excitation of each of the 12 vibrational modes in the equilibrium configuration have been determined. The results show that the total relaxation rate for each mode can be characterized with fair accuracy by a first-order rate law. Least-squares fitting of such a rate law to the computed data shows that the minimum decay rate among the 12 modes is significantly larger than the decomposition rate for vinyl bromide at an internal energy of 6.44 eV.[29] Such an inequality is a necessary condition to satisfy the basic assumption of statistical theories. However, it is also found that energy transfer is not globally rapid. Some modes are essentially inactive for over one picosecond. Consequently, it is possible that statistical theory will not adequately describe the decomposition processes occurring upon excitation of vinyl bromide.

Both the computed energy-transfer pathways and the total mode relaxation rate coefficients are found to be very sensitive to small variations in the surface curvatures near equilibrium and along the reaction coordinates. Some of the total relaxation rate coefficients for particular vibrational modes computed using PES1, PES2, and PES3 exhibit differences of more than a factor of 3. The differences between the ab initio potential and hybrid EPS surface can exceed a factor of 4. Therefore, we conclude that IVR rates for systems as complex as vinyl bromide computed using trajectory methods and ab initio potentials based on extensive electronic structure calculations will probably yield results with the correct order of magnitude but with errors that can be as large as a factor of 3. The sensitivity of the results to the fine details of surface curvature suggests that if total mode relaxation rates can be accurately measured, they will provide a very demanding test of potential-surface accuracy. In contrast, our previous investigations have shown that the computed unimolecular dissociation dynamics[29] do not exhibit such pronounced sensitivity to small variations in the reaction coordinate curvatures.

Finally, we have noted that although the more intimate details of intramolecular energy transfer are very sensitive to the fine details of the potential-surface curvatures, the gross behavior of the energy transfer dynamics is not. On all potential surfaces, the primary transfer processes are essentially the same and in all cases, the total energy transfer rate is found to be fast but not globally fast relative to the unimolecular dissociation rates of vinyl bromide.

References and Notes

(1) McDonald, J. D.; Marcus, R. A. *J. Chem. Phys.* **1976**, 65, 2180.
(2) Carter, D.; Brumer, P. *J. Chem. Phys*. **1977**, *77*, 4208.
(3) Sorbie, K. S.; Murrell, J. N. *Mol. Phys*. **1975**, 29, 6387.
(4) Foord, H.; Smith, J. G.; Whiffen, D. H. *Mol. Phys*. **1975**, 29, 1685
(5) Nagy, P. J.; Hase, W. L. *Chem. Phys. Lett*. **1978**, 58, 482.
(6) Stannard, P. R.; Gelbart, W. M. *J. Phys. Chem*. **1981**, 85, 3592.
(7) Sibert III, E. L.; Reinhardt, W. P.; Hynes, J. T. *J. Chem. Phys*. **1984**, 81, 1115.
(8) Pulay, P.; Fogarasi, G.; Boggs, J. E. *J. Chem. Phys*. **1981**, 74, 401.
(9) Sibert, E. L., III; Reinhardt, W. P.; Hynes, J. T. *J. Chem. Phys*. **1984**, 81, 1135.
(10) Uzer, T.; Hynes, J. T.; Reinhardt, W. P. *Chem. Phys. Lett*. **1985**, 117, 600.
(11) Uzer, T.; Hynes, J. T.; Reinhardt, W. P. *J. Chem. Phys*. **1985**, 85, 5791.
(12) Bintz, K. L.; Thompson, D. L.; Brady, J. W. *Chem. Phys. Lett.* **1986**, 131, 398.
(13) Guan, Y.; Thompson, D. L. *J. Chem. Phys*. **1988**, 88, 2355.
(14) Sumpter, B. G.; Thompson, D. L. *J. Chem. Phys*. **1987**, 86, 2805.
(15) Sumpter, B. G.; Thompson, D. L. *J. Chem. Phys*. **1987**, 86, 3301.
(16) Davis, M. J.; Gray, S. K. *J. Chem. Phys.* **1986**, 84, 5389.
(17) Davis, M. J. *J. Phys. Chem*. **1988**, 92, 3124.
(18) Kellerman, M. E.; Chen, G. *J. Chem. Phys*. **1991**, 95, 8671
(19) Kellerman, M. E. *J. Chem. Phys.* **1990**, 93, 5821.
(20) McCoy, A. B.; Sibert, E. L., III *J. Chem. Phys*. **1991**, 95, 3476.
(21) Martens, C. C.; Davis, M. J.; Ezra, G. S. *Chem. Phys. Lett*. **1987**, 142, 519.
(22) Marcus, R. A.; Hase, W. L.; Swamy, K. N. *J. Phys. Chem.* **1984**, *88*, 6717.
(23) Raff, L. M. *J. Chem. Phys*. **1988**, 89, 5680.
(24) Agrawal, P. M.; Sorescu, D. C.; Kay, R. D.; Thompson, D. L.; Raff, L. M.; Conrey, B.; Jameson, A. K. *J. Chem. Phys.* **1996**, 105, 2686.
(25) Pan, R.; Raff, L. M. *J. Phys. Chem.* **1996**, *100*, 8085.
(26) Pan, R.; Raff, L. M. *J. Chem. Phys*. **1997**, 106, 1382.
(27) Kay, R. D.; Raff, L. M. *J. Phys. Chem.* **1997**, *101*, 1007.
(28) Abrash, S. A.; Zehner, R. W.; Mains, G. J.; Raff, L. M. *J. Phys. Chem*. **1995**, 99, 2959.
(29) Rahaman, A.; Raff, L. M. *J. Phys. Chem., A* **2001**, *105*, 2156.
(30) Huzinaga, S.; Andzelm, J.; Klobukowski, M.; Radzio-Andzelm, E.; Sakai, Y.; Tatewaki, H. *Gaussian Basis Sets for Molecular Calculations*; Elsevier: Amsterdam, 1984.
(31) Osamura, Y.; Schaefer III, H. F.; Gray, S. K.; Miller, W. H. *J. Am. Chem. Soc*. **1981,** 103, 1904.
(32) Krishnan, R.; Frisch, M. J.; Pople, J. A.; Von R. Schleyer, P. *Chem. Phys. Lett.* **1981**, 79, 408.
(33) Smith, B. J.; Smernik, R.; Radom, L. *Chem. Phys. Lett*. **1992**, 188, 589.
(34) Halvick, Ph.; Liotard, D.; Rayez, J. C. *Chem. Phys*. **1993**, 177, 69.